

## Research Article

# Photoelectrocatalytic Degradation of Sodium Oxalate by TiO<sub>2</sub>/Ti Thin Film Electrode

Chen-Yu Chang,<sup>1</sup> Yung-Hsu Hsieh,<sup>2</sup> and Yu-Ying Chen<sup>2</sup>

<sup>1</sup> Center of General Education, National Taitung College, 889 Jhengci N. Rd., Taitung 95045, Taiwan

<sup>2</sup> Department of Environmental Engineering, National Chung Hsing University, 250 Kuo-Kung Road, Taichung 40227, Taiwan

Correspondence should be addressed to Chen-Yu Chang, cyc1136@ntc.edu.tw

Received 19 October 2011; Revised 18 December 2011; Accepted 19 December 2011

Academic Editor: Jiaguo Yu

Copyright © 2012 Chen-Yu Chang et al. This is an open access article distributed under the Creative Commons Attribution License, which permits unrestricted use, distribution, and reproduction in any medium, provided the original work is properly cited.

The photocatalytically active TiO<sub>2</sub> thin film was deposited on the titanium substrate plate by chemical vapor deposition (CVD) method, and the photoelectrocatalytic degradation of sodium oxalate was investigated by TiO<sub>2</sub> thin film reactor prepared in this study with additional electric potential at 365 nm irradiation. The batch system was chosen in this experiment, and the controlled parameters were pH, different supporting electrolytes, applied additional potential, and different electrolyte solutions that were examined and discussed. The experimental results revealed that the additional applied potential in photocatalytic reaction could prohibit recombination of electron/hole pairs, but the photoelectrocatalytic effect was decreased when the applied electric potential was over 0.25 V. Among the electrolyte solutions added, sodium sulfate improved the photoelectrocatalytic effect most significantly. At last, the better photoelectrocatalytic degradation of sodium oxalate occurred at pH 3 when comparing the pH influence.

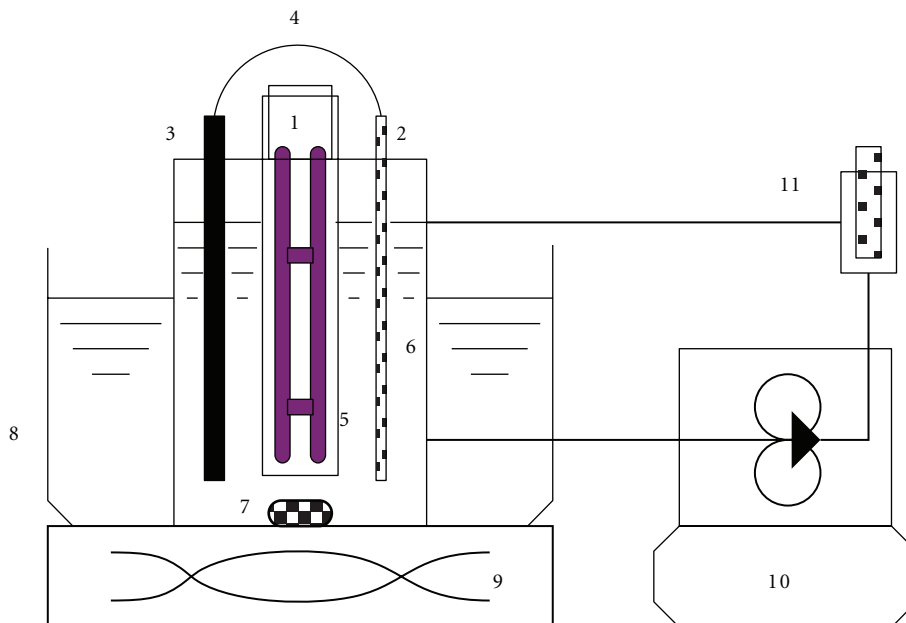
## 1. Introduction

Oxalic acid is frequently used in leather bleaching, chemical synthesis, printing and dye industries, rust removal, metal decontamination, and household bathroom cleaning. Therefore, cases of accidental oxalic acid poisoning are common. In addition, oxalic acid and its soluble salts can cause poisoning through the stomach and intestines, respiratory tract, skin, and eye contact with LD<sub>50</sub> between 375 and 475 mg Kg<sup>-1</sup>. Oxalate itself is also toxic to the kidney. In recent years, advanced oxidation processes have been extensively used in decomposing harmful or decomposition-resistant pollutants in the environment. Among them, the photocatalysis reaction using UV together with semiconductor is thought to be a treatment technology with high potential. Compared to other semiconductor metal oxides, titanium dioxide (TiO<sub>2</sub>) is the most frequently used photocatalyst for photochemical reaction due to the cheap cost, stable properties, and high photocatalytic effect. However, the recombination of electron-hole pairs occurs during the photocatalytic reaction process, resulting in the reduction of decomposition efficiency. In order to resolve such a problem for the increase of quantum efficiency, the following

approaches are frequently adopted: (1) application of a positive electric potential on the TiO<sub>2</sub> electrode to use the electric field force to drive away electrons in order to prevent further recombination; (2) combination of 2 semiconductors (such as TiO<sub>2</sub>/SnO<sub>2</sub>) at comparable energy levels to allow one (like SnO<sub>2</sub>) to absorb electrons during photoexcitation in order to improve decomposition efficiency; (3) addition of precious metal ions such as Ag or Pt in the reaction solution for the absorption for electrons [1–5]. This study used UV light of high energy to excite the photocatalyst to form hydroxyl radicals with high oxidizing ability to efficiently decompose organic pollutants in water in order to attain the goals of removal and mineralization [6–19].

## 2. Experimental Details

**2.1. Preparation of TiO<sub>2</sub> Photoreactor.** The modified chemical vapor deposition (CVD) [20] was used for the catalyst preparation used in the present study. The procedure is described as follows: The tetraisopropyl orthotitanate (Ti(OC<sub>3</sub>H<sub>7</sub>)<sub>4</sub>) (TTIP >98%, Merck Co.) solution and deionized water were placed in two aeration bottles separately. In the 60°C water bath, the aeration bottles were flushed with



(1) UV lamp, (2) anode (TiO<sub>2</sub>/Ti plates), (3) cathode (graphite), (4) external loop, (5) annular quartz tube, (6) reactor (pyrex), (7) magnetic stone, (8) water bath, (9) magnetic stirrer/hot plate, (10) circulating pump, and (11) pH meter.

FIGURE 1: Photoelectrocatalytic apparatus.

high-purity nitrogen gas to take out the airflow containing TiO<sub>2</sub> and water vapor. Teflon tubing was used on the other end into the reactor. The tubing was wrapped with heating tapes to approximately  $95 \pm 5^\circ\text{C}$  to avoid condensation. The substrate to be coated with the catalyst was placed in the tubular high-temperature oven to maintain the reaction temperature at  $400^\circ\text{C}$ . During the preparation, the formation of white smoke inside the reactor was observed with the naked eye, indicating that the TiO<sub>2</sub> crystal nucleus has started to grow on the wall of the tubing. The reactor was rotated to alter the position of the TiO<sub>2</sub> coating to allow it to coat evenly on the entire titanium substrate. Finally, the reactor was calcined at  $500^\circ\text{C}$  for 24 hours to eliminate impurities and purify TiO<sub>2</sub> to achieve the anatase as the major crystal form.

**2.2. Photoelectrocatalytic Procedure.** The liquid-phase photoelectrocatalytic system consisted of a UV lamp of 13 W and 365 nm, an annular reactor, a completely mixing chamber, a magnetic stirrer, a voltage supplier, and a circulating water bath. The apparatus is illustrated in Figure 1. In this study, the experiments were conducted in batches at constant temperature and sample volume. Other parameters including pH values, additional applied electric potentials, and the type of electrolytes were under control in the experiments (Table 1). 1 N HClO<sub>4</sub> and 4 N NaOH were used to adjust the pH value of aqueous samples. Besides, a peristaltic pump was used to draw sample into the reactor for the continuous refluxing batch experiments for 4 hours.

TABLE 1: Reaction conditions.

Conditions	Range
Water bath temperature	$20 \pm 1^\circ\text{C}$
The initial concentration of sodium oxalate	2 mM
Sample volume	350 mL
Flow rate	$300 \text{ mL min}^{-1}$
Refluxing time	4 hours
UV wavelength	365 nm
Irradiation intensity	$3 \text{ mW cm}^{-2}$
pH	3~7
Additional applied electric potentials	0, 0.25, 0.5, 1 V
Electrolyte solution (2 mM)	NaCl, NaNO <sub>3</sub> , Na <sub>2</sub> SO <sub>4</sub> , Na <sub>2</sub> CO <sub>3</sub>

**2.3. Quantitation of Species.** The relationships between the residual rates of sodium oxalate and the various controlled parameters were investigated in order to obtain the effect of TiO<sub>2</sub>/Ti thin film electrode. Ion chromatograph (IC; JASCO, Japan, Model PU-1580i) equipped with the Shodex IC SI-90-4E column and total organic carbon instruments (TOC; Shimadzu, Japan, Model TOC-VCSN) were employed for the analysis of the experiment to investigate the variations of the residual rates and the mineralization rates under parameters described above.

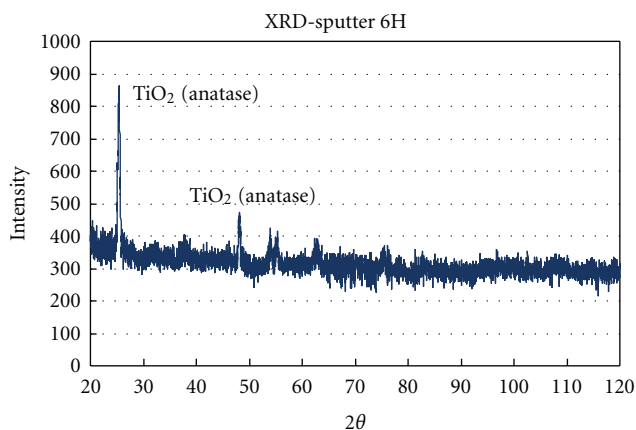


FIGURE 2: XRD spectrum of  $\text{TiO}_2$  prepared by CVD method.

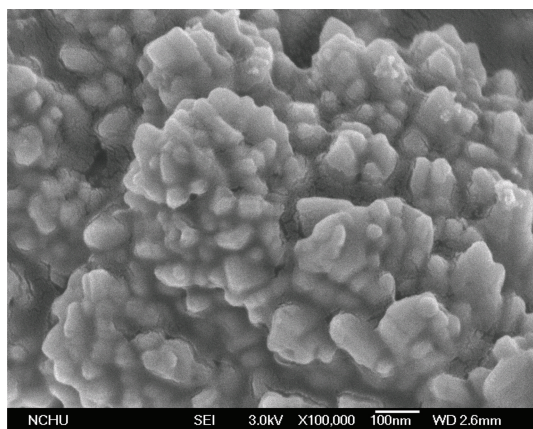


FIGURE 3: SEM image of  $\text{TiO}_2$  prepared by CVD method.

### 3. Results and Discussion

**3.1. Photocatalyst Properties.** The photocatalyst prepared by the modified CVD method under the optimal conditions described above was analyzed by the X-ray diffractometer (XRD) to examine the crystals form. As illustrated in Figure 2, the three major diffraction peaks of the anatase crystal structure appear at the  $2\theta$  values of 25.4 and 48.2; Compared with the JCPDS database (nos. 21-1276 and 21-1272), the crystal structure of the photocatalyst prepared in the experiment was mostly in the anatase form. The SEM image of the catalyst at magnification of 100,000 times illustrated in Figure 3, the structures of  $\text{TiO}_2$  particles were not rather uniform, with the appearance of clustered ball shape and the crystal surface of porous structure.

**3.2. Photoelectrocatalytic Tests.** Figure 4 shows the residuals of sodium oxalate in the  $\text{TiO}_2$  photocatalytic reaction alone, direct electrolysis alone, and photoelectrocatalytic process. It was clearly observed in the experimental data that at  $20^\circ\text{C}$ , pH 4, a volume flow rate of  $300\text{ mL min}^{-1}$ , and sodium oxalate of  $2\text{ mM}$  in the batch completely mixing reactor with the additional applied electric potential of  $1\text{ V}$  and the UV

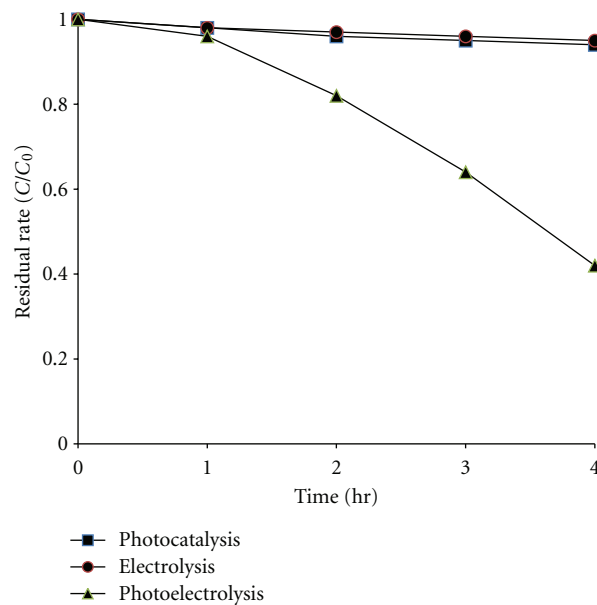


FIGURE 4: Residual rates of sodium oxalate under the different reactions at pH 4.

irradiation of  $365\text{ nm}$  for 4 hours for the photoelectrocatalytic degradation reaction experiment was able to increase the removal and mineralization rates of sodium oxalate from 6% to approximately 57%. According to Waldner's study, it was proposed that when  $\text{TiO}_2$  generated electron-hole pairs under UV irradiation, the additional applied electric potential inhibited the recombination of electron-hole pairs. The holes interacted with the water molecules or hydroxide ion ( $\text{OH}^-$ ) adsorbed on the surface of  $\text{TiO}_2$  to form hydroxyl radical ( $\cdot\text{OH}$ ), thus enhancing the oxidation reaction effect of holes [18, 19]. Moreover, according to the experimental results in Figure 5, it was observed that the mineralization rates of sodium oxalate had mostly comparable trends as the removal rate. It was suggested that the structure of sodium oxalate was rather simple, thus it was less likely to form intermediates. As a result, the degraded ones could be almost mineralized.

**3.3. pH Effect.** In general, as the pH of aqueous solution increases, the yield of hydroxyl radical in the photocatalytic reaction also increases. However, different pH values will directly affect the species distribution ratio of reactants in the solution. Moreover, pH values could also alter the surface electricity of photocatalyst, thus affecting the adsorption and desorption properties and abilities of reactants by the photocatalyst. Therefore, for different pollutants, the pH value controlled in the reaction could show a dramatic effect on the overall removal rate.

Figure 6 illustrated the residual rates of sodium oxalate at pH 3~7. The result indicated that sodium oxalate at  $2\text{ mM}$ , applied voltage of  $1\text{ V}$ , light intensity of  $3\text{ mW cm}^{-2}$ , volume flow rate of  $300\text{ mL min}^{-1}$ , temperature at  $20 \pm 1^\circ\text{C}$ , and UV light irradiation at  $365\text{ nm}$  on the titanium substrate plate coated with  $\text{TiO}_2$  in the reactor for 4 hours to undergo

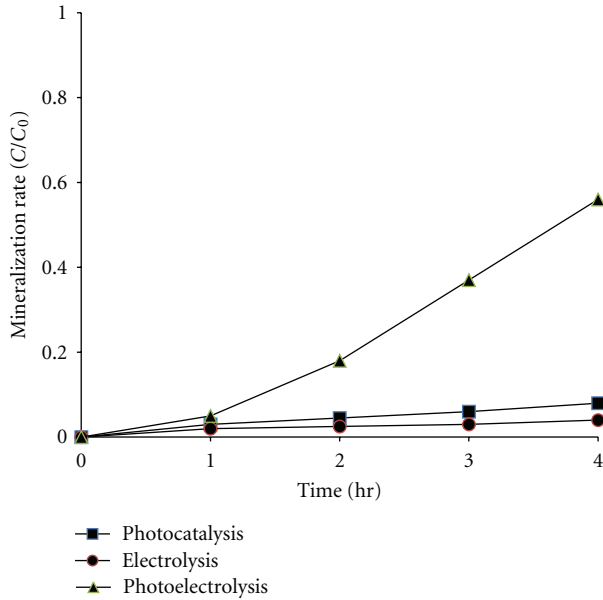


FIGURE 5: Mineralization rates of sodium oxalate under the different reactions at pH 4.

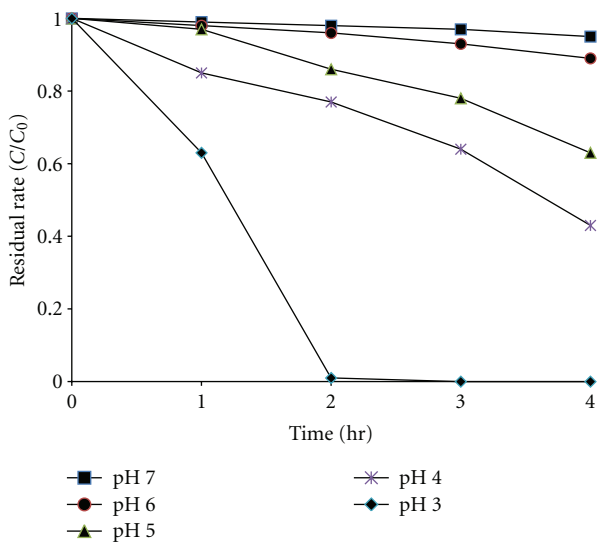


FIGURE 6: Residual rates of sodium oxalate under the photoelectrocatalytic reaction at different pH.

the photoelectrocatalytic reaction gave the most favorable treatment effect at pH 3. After a reaction for 150 minutes, the removal rate reached almost 100%. However, as pH values increased, the removal rate of sodium oxalate in the aqueous solution decreased. The cause of this phenomenon was probably that oxalate at the first ionization state ( $pK_{a1} = 1.2$ ,  $pK_{a2} = 4.2$ ) showed a more favorable reaction rate with  $\bullet\text{OH}$ . Furthermore, in the solid-liquid interface reaction, a low pH value was favorable for the adsorption of oxalate on the  $\text{TiO}_2$  surface, allowing the holes excited by  $\text{UV}/\text{TiO}_2$  to undergo the direct or indirect oxidation reaction in order to achieve goal of sodium oxalate degradation [19]. The

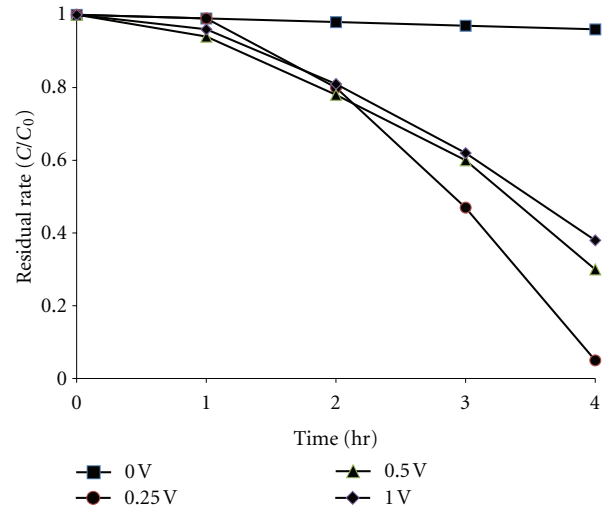


FIGURE 7: Residual rates of sodium oxalate under photoelectrocatalytic reactions with different additional applied electric potentials.

reason for the higher adsorption at lower pH was that the  $pH_{zpc}$  of  $\text{TiO}_2$  between 6.3~7.6 and the  $pK_a$  values of oxalic acid were approximately 1.2 and 4.2. As a result, when the pH value of the solution was higher than the  $pK_a$  of sodium oxalate but lower than the  $pH_{zpc}$  of  $\text{TiO}_2$ , sodium oxalate ionized a  $\text{Na}^+$  cation and formed  $\text{NaC}_2\text{O}_4^-$  with a negative charge. Meanwhile, the  $\text{TiO}_2$  surface carried a positive charge and a more favorable adsorption quantity was afforded due to the electrostatic attraction interaction between  $\text{TiO}_2$  and oxalic acid.

**3.4. Additional Applied Electric Potential Effect.** Figure 7 illustrates the results of the different additional applied electric potentials of 0.25 V, 0.5 V, and 1 V to the photoelectrocatalytic experiment of sodium oxalate. From the result shown, it was evident that the sodium oxalate removal effect was quite limited in the absence of the additional applied electric potential for the photocatalytic reactions. It was proposed that the electron-hole pairs excited by  $\text{UV}/\text{TiO}_2$  underwent the recombination reaction easily, leading to the consequence that the holes could not directly or indirectly oxidize organic substances. Consequently, the overall photocatalytic effect was reduced. However, the results of this experiment demonstrate that the additional applied electric potentials (0.25 V, 0.5 V, and 1 V) on the working electrode significantly improved the overall photoelectrocatalytic reactions. As the additional applied electric potentials varied, the degradation of sodium oxalate also varied to different degrees. Among them, the voltage of 0.25 V afforded a more favorable photoelectrocatalytic reaction. After 4 hours of the photoelectrocatalytic reaction, approximately 95% of sodium oxalate in the aqueous solution was removed. Nevertheless, when the additional applied electric potential was increased to 0.5 V, the sodium oxalate removal effect was lowered. Moreover, when it was increased to 1 V, the sodium oxalate removal rate was merely 57%. Therefore, the experimental results revealed that the applied voltage

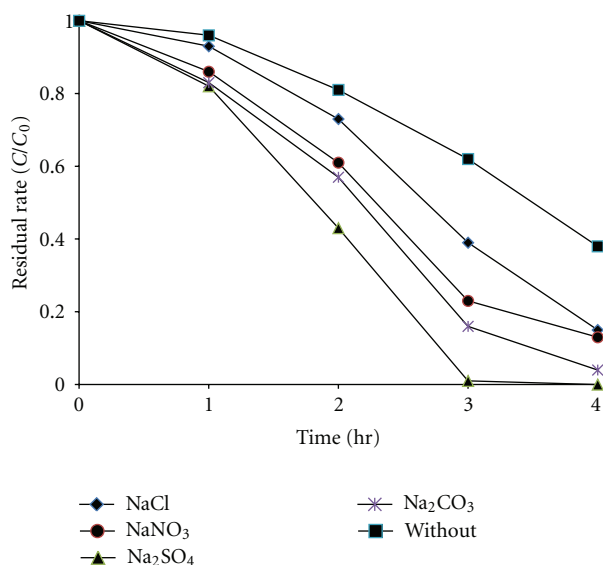


FIGURE 8: Residual rates of sodium oxalate under photoelectrocatalytic reactions with different electrolytes.

could reduce the recombination of electron-hole pairs, thus improving the overall removal effect. But, when an excess voltage was applied, the photoelectrocatalytic effect was worsened owing to the recombination reaction of the electrons of the additional applied electric potential itself and the holes carried on  $\text{TiO}_2$ .

**3.5. Electrolyte Solution Effect.** This experiment used sodium oxalate solution at an initial concentration of 2 mM followed by adding 0.2 mM of NaCl,  $\text{NaNO}_3$ ,  $\text{Na}_2\text{SO}_4$ , and  $\text{Na}_2\text{CO}_3$  electrolyte solution individually. The UV light at 365 nm was used to irradiate on the titanium substrate coated with  $\text{TiO}_2$  and the extra applied potential of 1 V was applied. The pH of the aqueous solution was controlled at  $4 \pm 0.1$  and the temperature at  $20 \pm 1^\circ\text{C}$  for the photoelectrocatalytic reaction in the complete mixing chamber for 4 hours to examine the effect of each electrolyte solution on the degradation of sodium oxalate. The results of this experiment are shown in Figure 8. The sodium oxalate degradation reaction the added electrolyte solution ( $\text{NaCl}$ ,  $\text{NaNO}_3$ ,  $\text{Na}_2\text{SO}_4$ , and  $\text{Na}_2\text{CO}_3$ ) was better than the one without the added electrolyte solution, indicating each electrolyte solution added was able to improve the photoelectrocatalytic reaction. Among them, adding  $\text{Na}_2\text{SO}_4$  showed the most favorable effect, with the sodium oxalate degradation rate reaching over 99% after 3 hours of operation time. The effects in the improvement of photoelectrocatalysis by different electrolyte solutions were found to vary in the order of  $\text{Na}_2\text{SO}_4 > \text{Na}_2\text{CO}_3 > \text{NaNO}_3 > \text{NaCl}$ . According to the study by Jorge, it was pointed out after adding different electrolyte solutions ( $\text{Na}_2\text{SO}_4$ ,  $\text{KNO}_3$ , and  $\text{NaCl}$ ) that  $\text{Na}_2\text{SO}_4$  was able to enhance the photoelectrocatalytic reaction to a greater extent, followed by  $\text{KNO}_3 > \text{NaCl}$ . This was because more photoelectric current was generated after adding  $\text{Na}_2\text{SO}_4$  to the system. The difference in the enhanced photoelectrocatalytic effects

from adding  $\text{Na}_2\text{SO}_4$  versus  $\text{NaCl}$  was found to be about over 10% [17]. This result was consistent with the conclusion of the present study.

## 4. Conclusions

The CVD method was used to prepare the  $\text{TiO}_2/\text{Ti}$  photocatalysis thin film reactor with the oxidation temperature controlled at  $400^\circ\text{C}$  and the calcination temperature at  $550^\circ\text{C}$  in this study. Not only the  $\text{TiO}_2$  purity was improved, but also the crystal structure was maintained at the anatase crystal form. Under the controlled parameters, the optimal experimental conditions were pH 3, 0.25 additional applied electric potential, and adding  $\text{Na}_2\text{SO}_4$  electrolyte in this study. The experimental results also showed that the effect of the photoelectrocatalytic process on the sodium oxalate removal efficiency was superior to that of the photocatalytic reaction alone. Moreover, it should be mentioned that the additional applied electric potential, in most cases, could enhance the overall degradation efficiency. However, the excessively high bias voltage could reduce the photocatalytic effect owing to the recombination of the electrons of the voltage itself and the holes carried on  $\text{TiO}_2$ . The search for the so-called “threshold dose” in the future study should be an attractive research subject.

## References

- [1] J. Yu, Y. Hai, and B. Cheng, “Enhanced photocatalytic  $\text{H}_2$ -production activity of  $\text{TiO}_2$  by  $\text{Ni}(\text{OH})_2$  cluster modification,” *The Journal of Physical Chemistry C*, vol. 115, no. 11, pp. 4953–4958, 2010.
- [2] W. C. Oh and M. L. Chen, “The improved photocatalytic properties of methylene blue for  $\text{V}_2\text{O}_3/\text{CNT}/\text{TiO}_2$  composite under visible light,” *International Journal of Photoenergy*, vol. 2010, Article ID 264831, 5 pages, 2010.
- [3] J. Yu, J. Xiong, B. Cheng, and S. Liu, “Fabrication and characterization of  $\text{Ag-TiO}_2$  multiphase nanocomposite thin films with enhanced photocatalytic activity,” *Applied Catalysis B*, vol. 60, no. 3-4, pp. 211–221, 2005.
- [4] J. Zhou, Y. Cheng, and J. G. Yu, “-light-driven plasmonic photocatalyst  $\text{Ag}/\text{AgCl}/\text{TiO}_2$  nanocomposite thin films,” *Journal of Photochemistry and Photobiology A*, vol. 223, no. 1-3, pp. 82–87, 2005.
- [5] Y. Li, G. Lu, and S. Li, “Photocatalytic transformation of rhodamine B and its effect on hydrogen evolution over  $\text{Pt}/\text{TiO}_2$  in the presence of electron donors,” *Journal of Photochemistry and Photobiology A*, vol. 152, no. 1-3, pp. 219–228, 2002.
- [6] C. Y. Chang, Y. H. Hsieh, L. L. Hsieh, K. S. Yao, and T. C. Cheng, “Establishment of activity indicator of  $\text{TiO}_2$  photocatalytic reaction-Hydroxyl radical trapping method,” *Journal of Hazardous Materials*, vol. 166, no. 2-3, pp. 897–903, 2009.
- [7] G. Shang, H. Fu, S. Yang, and T. Xu, “Mechanistic study of visible-light-induced photodegradation of 4-chlorophenol by  $\text{TiO}_{2-x}\text{N}_x$  with low nitrogen concentration,” *International Journal of Photoenergy*, vol. 2012, Article ID 759306, 9 pages, 2012.
- [8] Z. Zhang and J. Gamage, “Applications of photocatalytic disinfection,” *International Journal of Photoenergy*, vol. 2010, Article ID 764870, 11 pages, 2010.
- [9] J. A. Byrne, P. A. Fernandez-Ibañez, P. S. M. Dunlop, D. M. A. Alrousan, and J. W. J. Hamilton, “Photocatalytic enhancement

- for solar disinfection of water: a review,” *International Journal of Photoenergy*, vol. 2011, Article ID 798051, 12 pages, 2011.
- [10] J. Yu and B. Wang, “Effect of calcination temperature on morphology and photoelectrochemical properties of anodized titanium dioxide nanotube arrays,” *Applied Catalysis B*, vol. 94, no. 3-4, pp. 295–302, 2010.
- [11] J. Yu, G. Dai, and B. Cheng, “Effect of crystallization methods on morphology and photocatalytic activity of anodized TiO<sub>2</sub> nanotube array films,” *The Journal of Physical Chemistry C*, vol. 114, no. 45, pp. 19378–19385, 2010.
- [12] K. S. Yao, T. C. Cheng, S. J. Li et al., “Comparison of photocatalytic activities of various dye-modified TiO<sub>2</sub> thin films under visible light,” *Surface and Coatings Technology*, vol. 203, no. 5–7, pp. 922–924, 2008.
- [13] L. Zhao, J. Ran, Z. Shu, G. Dai, P. Zhai, and S. Wang, “Effects of calcination temperatures on photocatalytic activity of ordered titanate nanoribbon/SnO<sub>2</sub> films fabricated during an EPD process,” *International Journal of Photoenergy*, vol. 2012, Article ID 472958, 7 pages, 2012.
- [14] M. Zhou, J. Yu, S. Liu, P. Zhai, and L. Jiang, “Effects of calcination temperatures on photocatalytic activity of SnO<sub>2</sub>/TiO<sub>2</sub> composite films prepared by an EPD method,” *Journal of Hazardous Materials*, vol. 154, no. 1–3, pp. 1141–1148, 2008.
- [15] M. Y. Chang, Y. H. Hsieh, T. C. Cheng, K. S. Yao, T. C. Cheng, and C. T. Ho, “Photocatalytic degradation of 2,4-dichlorophenol wastewater using porphyrin/TiO<sub>2</sub> complexes activated by visible light,” *Thin Solid Films*, vol. 517, no. 14, pp. 3888–3891, 2009.
- [16] G. Dai, J. Yu, and G. Liu, “Synthesis and enhanced visible-light photoelectrocatalytic activity of p–N junction BiOI/TiO<sub>2</sub> nanotube arrays,” *The Journal of Physical Chemistry C*, vol. 115, no. 15, pp. 7339–7346, 2011.
- [17] S. M. Alves Jorge, J. J. de Sene, and A. de Oliveira Florentino, “Photoelectrocatalytic treatment of p-nitrophenol using Ti/TiO<sub>2</sub> thin-film electrode,” *Journal of Photochemistry and Photobiology A*, vol. 174, no. 1, pp. 71–75, 2005.
- [18] G. Waldner, M. Pourmodjib, R. Bauer, and M. Neumann-Spallart, “Photoelectrocatalytic degradation of 4-chlorophenol and oxalic acid on titanium dioxide electrodes,” *Chemosphere*, vol. 50, no. 8, pp. 989–998, 2003.
- [19] G. Waldner, R. Gómez, and M. Neumann-Spallart, “Using photoelectrochemical measurements for distinguishing between direct and indirect hole transfer processes on anatase: case of oxalic acid,” *Electrochimica Acta*, vol. 52, no. 7, pp. 2634–2639, 2007.
- [20] T. C. Cheng, K. S. Yao, Y. H. Hsieh, L. L. Hsieh, and C. Y. Chang, “Optimizing preparation of the TiO<sub>2</sub> thin film reactor using the Taguchi method,” *Materials and Design*, vol. 31, no. 4, pp. 1749–1751, 2010.



**Hindawi**

Submit your manuscripts at  
<http://www.hindawi.com>

